Available online at www.CivileJournal.org

Civil Engineering Journal

(E-ISSN: 2476-3055; ISSN: 2676-6957)

Vol. 9, No. 12, December, 2023

An Experimental Study of Strength Increase in Masonry Wall Reinforced by One-sided Khorasan Mortar with Steel Mesh

Volkan Öztaş [1*], Necdet Torunbalcı [1]

[1] *Faculty of Architecture, Istanbul Technical University, Istanbul, 34367, Turkey.*

Received 17 August 2023; Revised 18 November 2023; Accepted 23 November 2023; Published 01 December 2023

Abstract

The strengthening of masonry structures is of paramount importance due to their inherent lack of tensile elements, rendering them susceptible to tensile stresses induced by horizontal loads and the resultant substantial damage. Consequently, this study aims to develop a reinforcement system for the strengthening of historical masonry structures by using mortars devoid of cement and modern pozzolan. Experiments were conducted on masonry walls unreinforced and reinforced by a one-sided Khorasan mortar with steel mesh. Initially, six masonry brick walls constructed using Khorasan lime mortar were prepared. Subsequently, after a waiting period of six months, Khorasan plaster mortar, reinforced with steel mesh, was applied to three masonry walls on one side. Following an 18-month waiting period, all samples were subjected to testing in an experimental setup designed and manufactured for this purpose. The wall reinforcement resulted in a significant increase, with the average peak load by 215.73%, and the average displacement by 48.82%. The experimental shear force on unreinforced walls was found to be 41.23% lower than Eurocode-6 and 1.41% lower than TBDY-2018. In the case of one-sided reinforced walls, the experimental shear force was 9.94% lower than Eurocode-6 and 6.16% lower than TBDY-2018. This form of strengthening not only obviates the use of potentially damaging cement in historical buildings but also extends the lifespan of the reinforced structures.

Keywords: Khorasan Mortar; Masonry Wall; Steel Mesh.

1. Introduction

In Turkey, particularly in historical cities like Istanbul, numerous historical masonry structures continue to be in use. Many of these historic buildings exhibit a decrease in their load-carrying capacity over time due to factors such as corrosion caused by various reasons, including patterns of use and exposure to weather conditions, as well as inadequacies in renovation practices. To address these issues, various strengthening techniques have been developed and implemented to increase the structural and seismic performance of these structures. These techniques encompass a range of methods, including the use of fiber-reinforced (FRP) sheets and rods [1–3], textile-reinforced cementitious matrices (FRCM) [4, 5], composite-reinforced mortars (CRM) [6–8], and steel-reinforced plasters [9–11]. The primary objective of these methods is to augment the load-bearing capacity, ductility, and energy absorption capabilities of these structures, both in-plane and out-of-plane.

Biolzi et al. studied unreinforced and masonry walls with steel-reinforced plasters consisting of a thin layer of cementitious mortar or concrete (jacket) that incorporates a steel reinforcing mesh. The results of an experimental program of 13 confined masonry walls rehabilitated with different techniques are presented in the study. The walls were subjected to cyclic diagonal compression loading under displacement control. The results showed that the SRPs increased the performance of the walls considerably in terms of both strength and deformation capacity [9].

* Corresponding author: volkan.oztas@itu.edu.tr

http://dx.doi.org/10.28991/CEJ-2023-09-12-019

In the study conducted by Moeini et al., a cost-effective and straightforward repair/retrofit method known as steel-mesh reinforced shotcrete (SRS) is proposed. To substantiate the enhanced efficacy of this system, a series of experimental tests were carried out on typical 1:1.5 scale URM walls while considering influential parameters such as vertical loading, the presence of wall openings, and the impact of pre-existing damage in the URM. Initially, the walls were subjected to testing without any intervention to assess their response. Subsequently, the damaged walls were repaired using shotcrete on one side and subjected to another round of testing. Remarkably, the repaired/retrofitted walls exhibited improved performance, surpassing even the undamaged URM walls. The results indicate a significant improvement in lateral behavior, with an average increase of 288% in lateral strength capacity. Notably, the repaired walls performed on par with the corresponding retrofitted undamaged walls [10].

Warjri et al. present an experimental study of the structural behavior of masonry walls strengthened with steel-welded wire-mesh (WWM) overlayed with cement mortar to improve their in-plane shear strength and deformation capacity. The experimental program consists of a compression test of a masonry prism and a diagonal compression test of 15 wall specimens made of clay brick strengthened with four different WWM systems: (i) embedding WWM along the bed joint; (ii) embedding WWM along the bed joint and a strip diagonally crossing the wall surface; (iii) embedding WWM alternately along the bed joint, continuing to the surface of the wall; and (iv) WWM fully covered on the wall surface. The experimental results show that the adopted WWM-strengthening solutions produce a beneficial increase in compressive strength, shear resistance, ductility, and energy dissipation capacity, making them suitable for seismic strengthening [11].

Ullah et al. present the seismic performance of brick masonry strengthened with steel and plastic meshes. For this purpose, twenty masonry wallets were constructed, keeping the same materials and workmanship. Fifteen of them were reinforced using steel and plastic meshes. These specimens were tested for in-plane static cyclic diagonal tension (shear) behavior. The critical parameters, such as shear stress, strain, failure modes, ductility, energy dissipation, and stiffness degradation, were investigated. Compared to reference and plastic-reinforced specimens, the steel-reinforced brick samples with cement mortar were found to be highly effective [12].

In the study conducted by Lubin et al., the results of an experimental program involving 13 confined masonry walls rehabilitated with various techniques are presented. All specimens were constructed at full scale with an aspect ratio (height to length) of 1. In one of the walls, the vertical confining elements were constructed using 6.4 mm-diameter welded wire reinforcing cages. Before the rehabilitation phase, 11 out of the 13 walls were initially subjected to testing to induce repairable damage, while the other 2 were strengthened in their undamaged state. Throughout the testing, the walls were subjected to a constant vertical load. Initially, the damaged walls were rehabilitated using various techniques, such as jacketing with cement mortar, welded wire mesh, and synthetic or steel fibers. Additionally, one of the initially damaged walls was rehabilitated using premixed mortar and fiberglass mesh. Following the rehabilitation, the specimens were tested to assess their failure behavior. The results indicated a significant increase in the original capacity of the walls in terms of strength, stiffness, and deformation using the studied techniques [13].

Hasnat et al. present an experimental investigation on the behavior of an in-plane-loaded Unreinforced Masonry (URM) wall retrofitted with ferrocement technology. Quasi-static cyclic tests were conducted on full-scale URM walls. The unreinforced masonry walls were constructed using clay bricks and positioned on a reinforced concrete base slab. The walls were subjected to a thorough ferrocement overlay, including additional joint lamination between the base slab and the wall panel. Steel wire meshes with an opening size of 12.5×12.5 mm were considered for the ferrocement overlay. The behavior of the strengthened walls under a combination of vertical load and lateral reversed cyclic loading was compared to the control models to assess the improvement in lateral load resistance capacity. The presence of ferrocement significantly enhanced the post-cracking strength, increasing it by nearly 1.6 times the failure load. The principal finding of this test is the demonstration of the substantial post-cracking strength and displacement capacity of URM walls with ferrocement lamination [14].

In Şimşek's study conducted in 2018, four series of mortar samples were prepared to determine the mixing ratios of the masonry mortar for use in fabricating model brick walls and plaster mortar for reinforcing the resulting samples. Following the determination of the mortar mixing ratios for the experimental study, model brick walls measuring 200 mm x 200 mm were manufactured. Diverging from conventional experimental studies that employ cement mortar, these model brick walls were reinforced with textile and steel-mesh-reinforced lime-based Khorasan mortar. The study involved determining the mechanical properties of lean and reinforced model brick walls through diagonal pressure testing. The findings revealed that brick walls with reinforced mortar exhibited higher ultimate loads, shear stresses, and deformation capacities when compared to unreinforced model brick walls [15].

The study conducted by Torunbalcı et al. involved experimental investigations into the behavior of brick masonry wall samples reinforced on one side with self-compacting concrete and standard concrete. Additionally, it includes a pivotal case study illustrating the application of these reinforcement methods to historical structures. Comparisons were made between the alterations in the load-bearing capacities and the behavior of the specimens following the strengthening. The results indicated that the improvements in the samples were significantly more pronounced when self-compacting concrete was utilized, in contrast to conventional concrete reinforcement [16].

The study conducted by Torunbalcı et al. focused on experimental investigations into the strengthening of masonry structures, particularly historical structural walls, which are often feasible to reinforce on one side. In the experimental works conducted within the scope of the study, the brick wall specimens, including some that were pre-damaged, were reinforced on one side using cement mortar and carbon-fiber-reinforced polymers (CFRPs) in various forms. Comparative assessments were made to analyze the changes in the load-bearing capacities and behaviors of the specimens following the strengthening. The findings revealed that unreinforced brick wall specimens exhibited brittle behavior, whereas the performance of the brick wall specimens reinforced with CFRPs exhibited improvements in terms of strength ratings and energy dissipation capacities. Notably, the enhancements in the structural brick wall specimens were more significant when the reinforcement was applied to the entire surface of the wall in textile form rather than in strip form [17].

Garcia et al. conducted an experimental investigation to examine the behavior of masonry walls reinforced with single- and double-layer steel-reinforced lime mortar (SRG). They performed cyclic shear pressure tests on walls reinforced with lime mortar consisting of low-density steel cords (LDS). Lime mortar was applied on both sides of the walls in a strip configuration, utilizing one and two layers of LDS. The inclusion of SRG with a single layer of LDS facilitated the proper redistribution of stresses throughout the strips, enabling the specimens to withstand larger imposed loads and displacements. This outcome underscores the effectiveness of the strengthening technique [18].

Wang et al. conducted an experimental investigation focused on the in-plane shear behavior of grey clay brick masonry panels that were strengthened with steel-reinforced grout (SRG), which is produced by embedding high-strength steel cords within a cementitious mortar matrix. Diagonal compression tests were carried out on a total of eight panels, comprising two unreinforced panels and six strengthened panels with different reinforcement configurations. The contribution of the SRG system to strengthening was assessed by evaluating the shear stiffness, shear strength, ductility under shear, and changes in failure mechanisms. The results demonstrated that SRG strengthening of masonry panels significantly enhances their in-plane behavior, as reflected in improvements in shear stiffness, shear strength, and ductility under shear [19].

In the study conducted by Özsaraç, the impact of employing woven Glass Fiber Reinforced Polymer (GFRP) material for reinforcing masonry brick walls with pozzolanic cement mortar was investigated, exploring various forms and quantities of reinforcement and their effects on strength and ductility. The strengths of the model brick walls reinforced with GFRP were assessed through diagonal pressure tests and compared to the values of the unreinforced model brick walls. The data obtained from the experiments were analyzed, revealing that the most substantial increase in strength resulted from using GFRP reinforcement that covered the entire surface. There was also a significant enhancement in strength with GFRP reinforcement in strip form. Moreover, it was observed that the model walls reinforced on one side displayed a substantial increase in both strength and ductility [20].

Son et al. investigate the enhancement of the in-plane strength and ductility of UMWs using GFRPU, depending on the shape of the GFRPU coating on the wall. Four masonry wall specimens are tested with test variables of the number of strengthening sides and coating shapes. It is illustrated that the Glass-Fiber-Reinforced Polyurea (GFRPU) reinforcement of masonry walls leads to enhanced load-carrying capacity, ductility, and energy absorption. An empirical formula to represent the degree of strengthening affected by GFRPU was created [21].

In the study of Khan et al., the computational modeling of Dry-Stack Block Masonry (DSM) walls subjected to cyclic monotonic loading testing is done. The analytical results were compared with experimental test results of the unreinforced and unconfined DSM cantilever walls subjected to lateral loading along with a constant axial load. ABAQUS has been used for Finite Element Modeling and analysis of the wall. Various material properties are defined for the wall in the software and modeled as a homogeneous material. The proposed numerical models had a good correlation with the experimental data [22].

ElGawady et al., in their experimental study, investigated the in-plane seismic behavior of URM walls before and after retrofitting using fiber-reinforced polymers (FRP). The specimens were retrofitted on one side using different types and structures of FRPs. Subsequently, the test specimens were subjected to a series of synthetic earthquake motions on a uni-axial earthquake simulator. The retrofitting technique improved the lateral strength and stiffness of the URM walls. Moreover, the fundamental frequency and the initial stiffness of each specimen remained relatively constant before and after retrofitting. During the testing, the slender specimens exhibited failure in flexural behavior. For specimens that failed in flexure, the measured FRP axial strains showed that the strain distributions along the specimens' cross-sections were approximately linear even at failure. Consequently, the flexural strengths of the specimens were calculated using the linear elastic approach. The measured lateral resistances of slender specimens were approximately 130% of the calculated flexural strength. This difference can be attributed to variations in the nominal ultimate strains of FRPs compared to their actual values at failure. The measured axial strains in FRPs during this test were approximately 50% of their nominal values. Additionally, the shear strengths of the squat specimens were calculated using two different models, resulting in calculated shear strengths ranging from approximately 99% to 177% of the measured lateral resistances [23].

In the study of Ismail et al., the structural performance of historical masonry wall (URM) systems reinforced with two different textile polymer (TRM) materials was investigated. The testing was performed in two series, with series 1 involving in-plane testing of two pier-spandrel assemblages representing part of a perforated URM wall and series 2 involving out-of-plane testing of three slender walls having no penetrations. To replicate the physical characteristics of historic masonry materials, vintage solid clay bricks and a low-strength hydraulic cement mortar were used for the construction of the test walls. Numerous structural characteristics pertaining to the seismic behavior of TRM-strengthened historic URM walls were investigated and then compared to those obtained from corresponding as-built tested URM walls. In general, strengthened walls exhibited ductile behavior until the polymer textile ruptured in a brittle manner. The strength increments due to TRM strengthening were observed to range from 128% to 136% when the URM test walls were loaded in-plane and from 575% to 786% when the URM test walls were loaded out-of-plane [24].

In the experimental study of Shermi et al., they investigated the masonry behavior of double-sided reinforced masonry walls with mesh reinforcement and cement-coarse sand mortar as reinforcement materials. This experimental study aims to investigate the behavior of URM and URM strengthened with welded wire mesh (WWM) as reinforcing material and 1:3 cement coarse sand mortar. A series of six unreinforced masonry (URM) panels and 18 reinforced panels were constructed using two different types of mortar and subjected to diagonal axial compression tests. Three types of WWM that are locally available on the market have been used in this study. Test results show a significant increase in strength and ductility, with useful suggestions for the practical utilization of this technique. The shear strength of the reinforced samples reached approximately four times that of the unstrengthened samples [25].

Section eleven of the Turkish Building Earthquake Code of 2018, titled “Special Rules for the Design of Masonry Carrier Systems under the Impact of an Earthquake”, delineates the regulations for the earthquake-resistant design and construction of unreinforced, confined, and reinforced masonry buildings, as well as reinforced panel system buildings to be constructed in seismic zones. This section stipulates that all joints, both horizontal and vertical, in load-bearing masonry walls must be filled with binder mortar. Furthermore, it provides essential information regarding the characteristic compressive strength of load-bearing masonry walls and the initial shear strength of these walls, aimed at facilitating the design process [26].

The ASTM E519/E519M-15 Standard Test Method for Diagonal Tension (Shear) in Masonry Assemblages standard outlines the procedure for applying pressure loading to 120 × 120 cm test specimens in the cross direction, with the objective of determining tensile and compressive strengths. Within this standard, it is recommended to prepare a minimum of three specimens for each type, ensuring the use of the same type of brick, mortar, and workmanship. The prepared samples should remain stationary for a duration of seven days and be stored within a laboratory environment for a minimum of 28 days. The recommended laboratory conditions specify a temperature range of 24 ± 8°C and a humidity range of 25-75% [27].

In Turkey, numerous historical masonry structures remain in use, particularly in historical cities such as Istanbul. Within these structures, the load-carrying capacity may decrease due to deterioration over time or improper interventions resulting from modifications. These issues can be addressed through various strengthening methods [28, 29].

This study aims to develop a reinforcement system for the strengthening of historical masonry structures using mortars devoid of cement and modern pozzolans. This approach to strengthening mitigates the use of materials such as cement, which can potentially harm the existing bricks and mortars in historical buildings, thereby ensuring extended longevity for the strengthened structures. Consequently, an experimental study was carried out on masonry walls to devise a strengthening system using cement and mortars that do not contain modern pozzolans for reinforcing historical masonry structures. In this context, systems similar to the Khorasan mortar and filled brick wall, originally implemented in historical buildings, were fabricated. Subsequently, some of these samples underwent strengthening, and the resulting increases in strength were determined. The intermediate mortar used in masonry is a non-cement-based mortar tailored for the historical Khorasan mortar. Additionally, the mortar's composition for reinforcement omitted the use of cement, incorporating pozzolans and binders compatible with historical structures instead.

The ASTM E519/E519M-15 standard also guided the design of the wall sample dimensions. In accordance with the provisions of this standard, three specimens of each sample type were fabricated using the same size, type of brick, mortar, and workmanship. Among these specimens, three of them are unreinforced walls, and three of them are one-sided reinforced walls. Samples of 150 × 150 cm were prepared in sizes larger than the minimum wall dimensions of 120 x 120 cm specified in the standard [27].

Cement-containing mortars have negative effects on masonry bricks and brick combination mortars. The rapid setting time limits the time available to the user to work with the gauged mortar. Some types of cement contain appreciable amounts of soluble salts, particularly potassium sulphate, which may become a source of salt damage to stonework. The use of cement tends to lead to the user treating the gauged lime mortar as if it were fully hydraulic lime or cement. Too much reliance on the initial chemical set leads to a negligence of the importance of the longer-term carbonation of the non-hydraulic component present. The danger is that segregation occurs, whereby the cement separates from the lime as the mortar dries and hardens [28–30].

Due to these negative effects, studies on the use of cement-free lime-based mortars in strengthening masonry walls are gaining importance. It is important to use high-quality lime and pozzolana to increase the strength of lime-based mortars. Additionally, adding steel mesh reinforcement to lime-based reinforcement mortars increases the ductility and strength of masonry walls. With this study, we tried to fill the gaps in the literature regarding the strengthening of masonry walls with lime-base mortar with steel mesh.

The in-plane behavior of masonry walls reinforced by uncemented lime plaster with steel mesh is the focus of this study. This study aims to develop a reinforcement system for the strengthening of historical masonry structures by using mortars with steel mesh. Therefore, an experimental study was carried out on masonry walls for the development of a strengthening system. The research flow chart is shown in Figure 1.

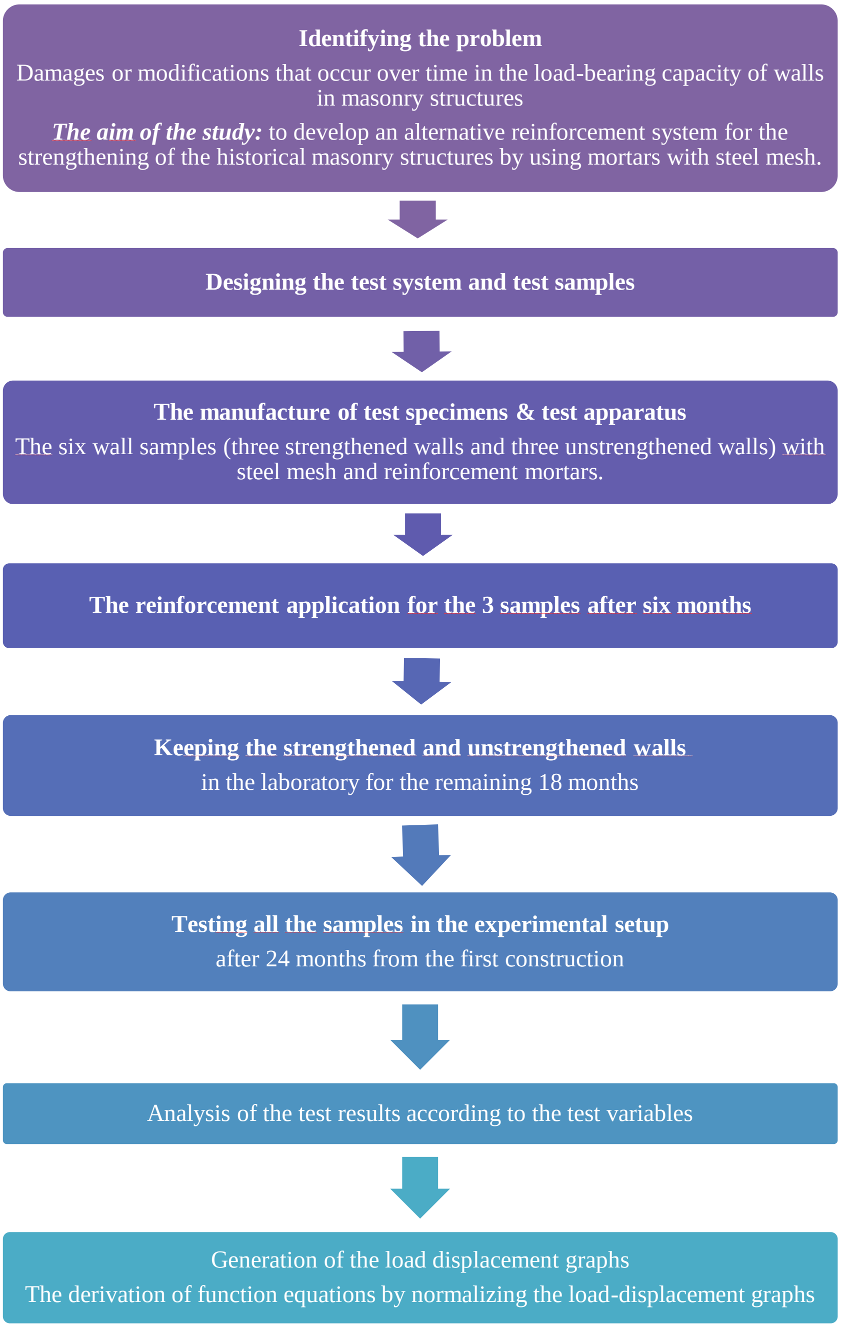

Figure 1. Flowchart of this study

2. Experimental Program

In the experimental study, the process began with the design and fabrication of the experimental setup. Subsequently, wall samples were produced and kept in the laboratory for the necessary duration. Finally, all samples underwent testing within the experimental setup, and the results were evaluated.

2.1. Test Specimens

For the experimental study, six wall samples were constructed. During the construction of these walls, two types of mortar samples were prepared, tailored to suit solid blend bricks, and historical mortars were used. The ratios of masonry mortar and reinforcement mortar used for the wall samples were derived from Şimşek's study. The ratios of masonry mortar and reinforcement mortar used for the wall samples were derived from Şimşek's study. In this context, the masonry mortar ratios from the mentioned study were adopted for the mortar to be used between the bricks, while the reinforcement mortar ratios were used for the mortar applied to the brick surface [15].

In the mortar production process, 4 mm river sand and 4 mm brick fragments were used as aggregates. The binder consisted of natural hydraulic lime and trass (a natural pozzolan). Natural hydraulic lime is a type of lime well-suited for mortars to be used in historical buildings that do not contain cement or other binding materials [15]. Trass extracted from the Istanbul Sile region was used as the pozzolan. Tables 1 and 2 present the ratios of the components in the Khorasan joint mortar and reinforcement mortar used in the experimental study.

Table 1. Khorasan joint mortar rates by weight

	Weight (kg/dm^3)	Percentage rate (%)	Weights of mortar components to be used for a masonry sample (kg)	Weights of mortar components to be used for a masonry sample (g)
Brick Ballast (4 mm)	1,054	42,08	43,81	43813,1
Trass	0,275	10,96	11,41	11410,5
River Sand (4 mm)	0,638	25,47	26,52	26520,6
Hydraulic Lime	0,139	5,53	5,76	5757,2
Water	0,400	15,97	16,63	16627,4
Total	2,505	100,00	104,13	104128,8

Table 2. Khorasan plaster mortar rates by weight

	Weight (kg/dm^3)	Percentage rate (%)	Weights of mortar components to be used for a masonry sample (kg)	Weights of mortar components to be used for a masonry sample (g)
Brick Ballast (4 mm)	0,53	18,97	30,05	30.049,24
Trass	0,55	19,76	31,30	31.303,67
River Sand (4 mm)	0,64	22,97	36,38	36.378,40
Hydraulic Lime	0,55	19,94	31,59	31.588,77
Water	0,51	18,36	29,08	29.079,91
Total	2,78	100,00	158,40	158.400,00

Solid blend bricks of size 19×9×5 cm produced in Çorum-Türkiye were used in the construction of the walls. These bricks have more irregular surfaces and corner formations than modern bricks produced with smooth surfaces. Therefore, it was preferred to use them as the brick types with the closest features to the brick types in historical buildings.

During the preparation of the sample walls, a reinforced concrete foundation measuring 25×25×150 cm was constructed for the lower part of the masonry wall. A sufficient amount of steel reinforcement was incorporated into the foundation to address the stresses generated from the wall loading. This foundation served a dual purpose by not only facilitating the transportation of the wall specimens to the experimental setup but also ensuring a uniform load distribution on the lower parts of the wall during the experiment.

On these foundations, masonry walls with dimensions of 150×150 cm, 9 cm thickness, and joint gaps of approximately 2 cm horizontally and 2 cm vertically were built with filled blend bricks and the prepared masonry mortar. Knitting mortar was used in all joints, both horizontally and vertically.

Out of the six samples produced, three were kept in the laboratory environment for two years without strengthening. Following a six-month waiting period, the remaining three samples had mesh steel applied to one surface, followed by the application of a 4 cm sprinkling of reinforcement mortar. Subsequently, the strengthened samples, along with the non-reinforced ones, were kept in the laboratory environment for an additional 18 months. All samples underwent testing within the experimental setup after being maintained in a laboratory environment for a total of 24 months, beginning from the first construction.

The wall samples were coded into two groups according to their reinforcement types. A code-sample number system was used. The abbreviations for coding are as follows;

- D: Unreinforced wall

- TGD: One-sided reinforced wall
- Sample number: 1-2-3

Sample codes were formed as D1 - D2 - D3 - TGD1 - TGD2 - TGD3 respectively. Figures 2 and 3 show examples of unreinforced wall specimens and one-sided reinforced wall specimens in the laboratory environment.

Figure 2. Unreinforced wall specimen

Figure 3. One-sided reinforced wall specimen

Mesh steel reinforcement with the code Q84/84, 4 mm bar diameter, 150×150 mm mesh spacing was used as reinforcement on the samples to be strengthened. The reinforcements were cut as 150×150 cm in accordance with the wall dimensions.

For the wall samples designated for single-surface strengthening, anchorage holes were drilled to a depth of approximately 5-6 cm, b aligning them with the marked anchorage locations and the steel-mesh in both the horizontal and vertical orientations. L-shaped anchor pieces were crafted from the steel mesh, ensuring its integration with the wall. These anchors were fashioned in an L-shape, measuring a total of 12 cm, composed of 8 cm + 4 cm segments. The interior of the anchor holes was cleaned with a compressor, followed by the application of epoxy within the holes. Anchors were inserted in the holes simultaneously with the epoxy application. Once the anchors achieved sufficient strength, the steel-mesh reinforcements, tailored to the wall's dimensions, were fastened to the anchors with binding steel (Figure 4).

Figure 4. Steel-mesh and anchor application on the wall surface

Anchors and reinforcements were placed at a distance of 2 cm from the wall so that the reinforcement mortar could fully cover the reinforcements. It was planned to apply the thickness of the reinforcement mortar as 4 cm. A 4-cm-thick reinforcement mortar was applied to the surface of the reinforced walls (Figure 5).

Figure 5. A 4-cm-thick reinforcement mortar application on the wall surface

2.2. Test Setup

In this study, a reaction frame was designed for the static loading of the wall samples to be built first. The main carrier system, the system formed with HEB260 profiles, can withstand loads up to approximately 800kN. The test frame is designed in dimensions to allow the testing of samples of various sizes. With the bolted system, the frame is made suitable for attaching additional parts. With various support profiles, the experimental setup can be strengthened to withstand larger loads in different directions (Figure 6).

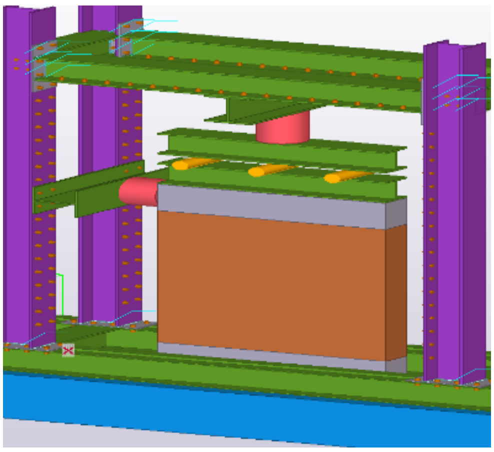

Figure 6. Designed test setup

The experimental setup is equipped with two hydraulic loading cylinders. The hydraulic cylinder affixed to the horizontal profiles on the upper part of the experimental setup was used for consistent vertical downward loading. This roller applies loads such as dead/moving loads from the floor, distributed loads from the upper floor walls onto the lower floor wall, etc. It is used to apply the loads stemming from various building elements. The second hydraulic loading cylinder is positioned horizontally between the vertical profiles, aligning with the upper level of the samples for horizontal loading. Directly beneath the vertical hydraulic cylinder, two HEB240 horizontal profiles, each measuring 150 cm in length, are arranged to match the sample dimensions. Cylindrical steel pieces with a 5 cm diameter are placed between these profiles. This configuration allows the upper part of the sample to act as a sliding support, enabling free movement during horizontal loading. In order to adjust the height of this sliding support system, a pair of motors with a load capacity of 250 kg are installed on the upper part of the experimental setup. This mechanism is raised before the sample is positioned, facilitating the sample placement process and accommodating height adjustments for differently sized samples (Figure 7).

Figure 7. Produced test setup

2.3. Loading and Measuring System

The measurement system includes one diagonal and four horizontal displacement meters. Displacement gauges k1 and k2 are positioned on the loading side, while displacement gauges k5 and k6 are situated on the opposite side. In this configuration, the displacement meter k4 is placed diagonally. The setup utilizes one horizontal and one vertical hydraulic cylinder are used. A constant distributed load of 33.3 kN/m is applied using a vertical hydraulic cylinder (Figure 8).

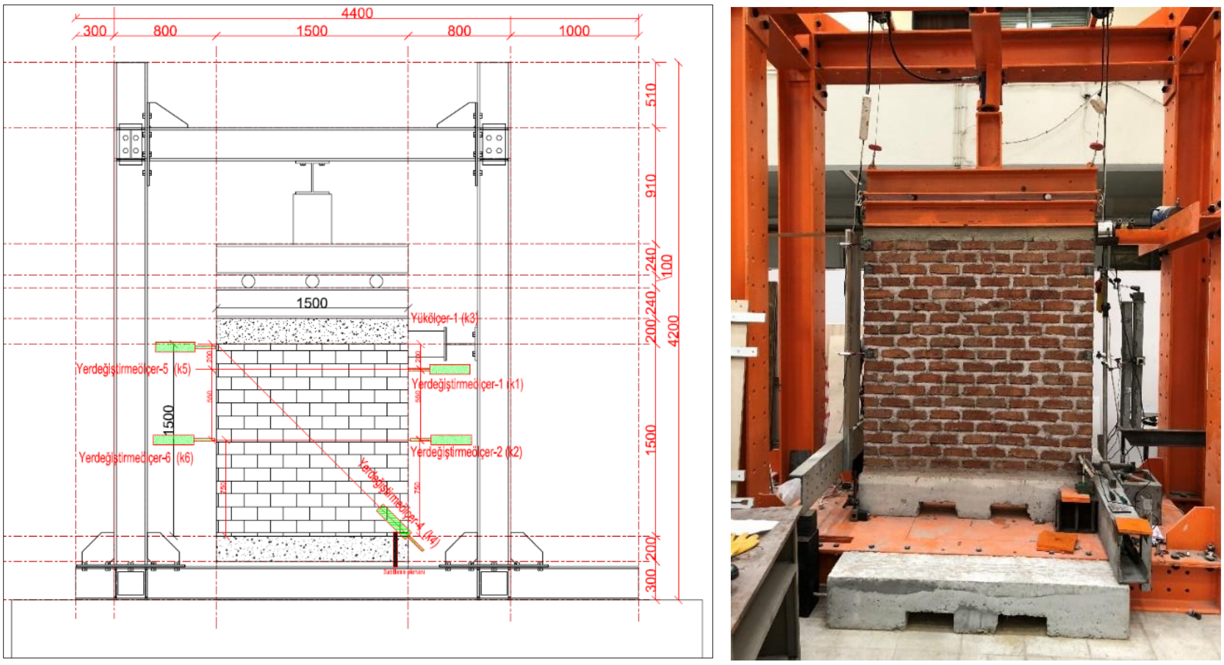

Figure 8. Test setup and sample placement

3. The Fracture Shapes and Load-Displacement Graphics

First of all, the tests of the unreinforced wall samples were carried out. Diagonal fractures were observed as a result of the loading test in all three wall samples (Figure 9).

a) D1 wall

b) D2 wall

c) D3 wall

Figure 9. Fracture patterns of unreinforced walls

The fracture state of the D1 wall sample differed compared to the D2 and D3 wall samples. During the loading of the D1 wall specimen, the diagonal fracture occurred slowly. The displacements k1 and k2 on the loading side of the sample exhibited significant plastic behavior even after the diagonal fracture, and preserved the wall displacement in this region. In contrast, during the loading of the D2 and D3 wall samples, the diagonal fracture occurred suddenly. The k1 and k2 displacements on the loading side of the sample exhibited highly elastic behavior after diagonal fracture. Unlike the other displacements, the wall displacement and the initial displacements came to close values (Figure 10).

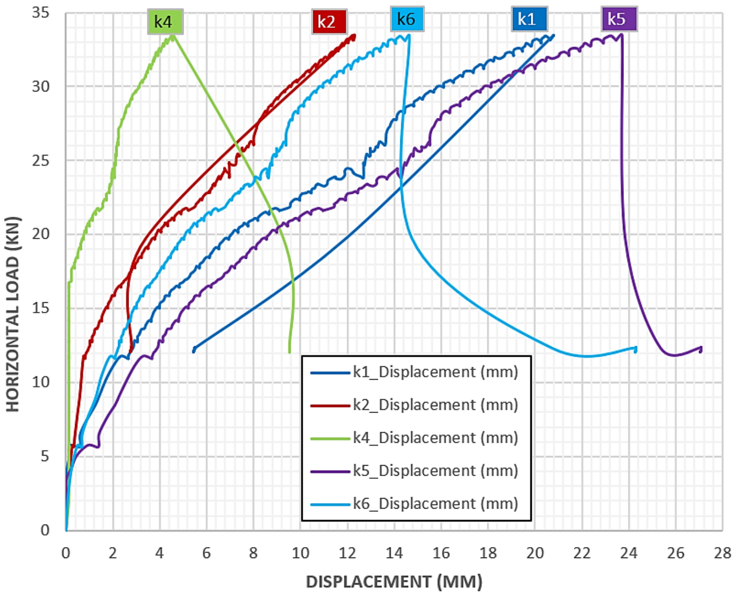

a) D1 wall

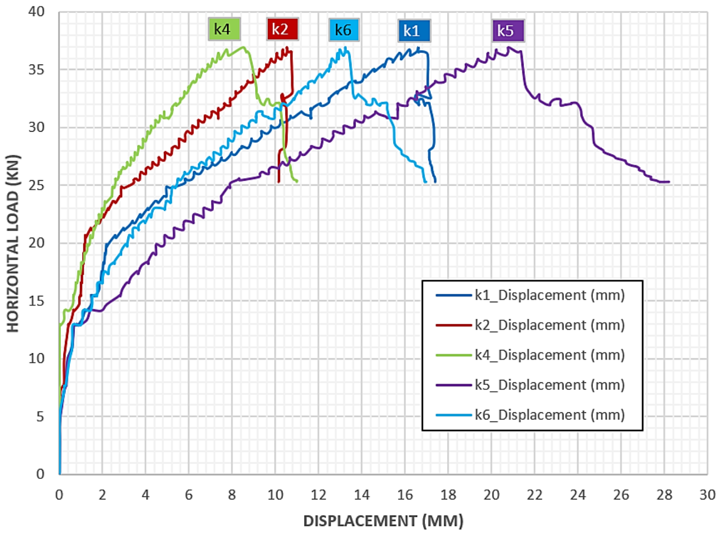

b) D2 wall

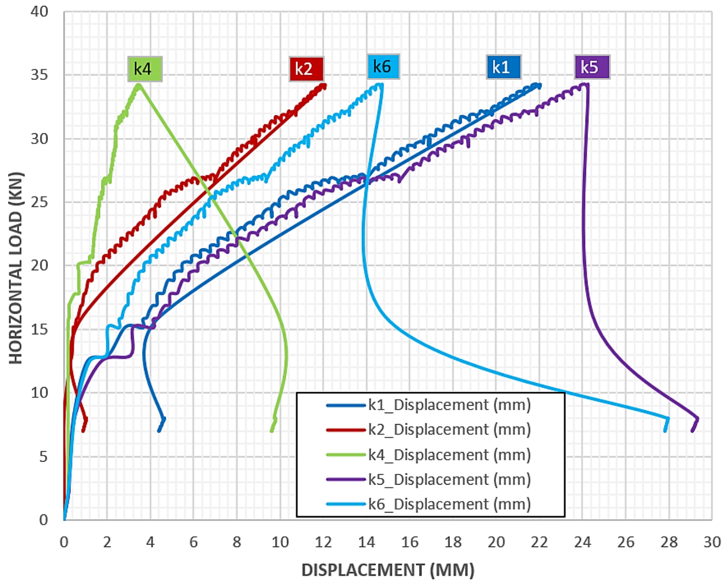

c) D3 wall

Figure 10. Horizontal load - displacement graphics for unreinforced walls

The single-sided reinforced wall specimens exhibited similar fracture behavior. It was observed that a diagonal fracture occurred on the non-reinforced surface, while grid cracks formed on the mesh reinforcement lines of the reinforced surface (Figures 11, 12, and 13). Horizontal load-displacement graphics for one-sided reinforced walls are presented in Figure 14.

a) Front side

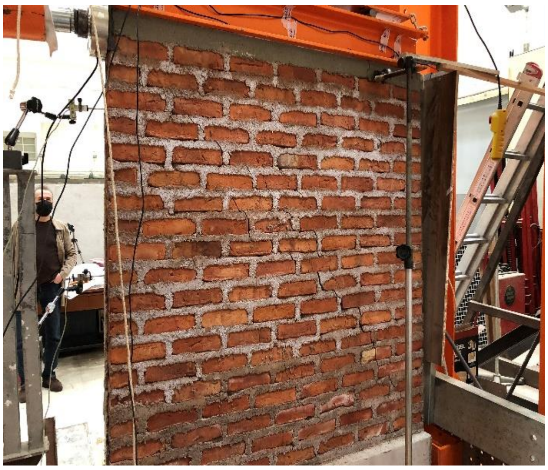

b) Back side

Figure 11. TGD1 wall fracture patterns

a) Front side b) Back side

Figure 12. TGD2 wall fracture patterns

a) Front side b) Back side

Figure 13. TGD3 wall fracture patterns

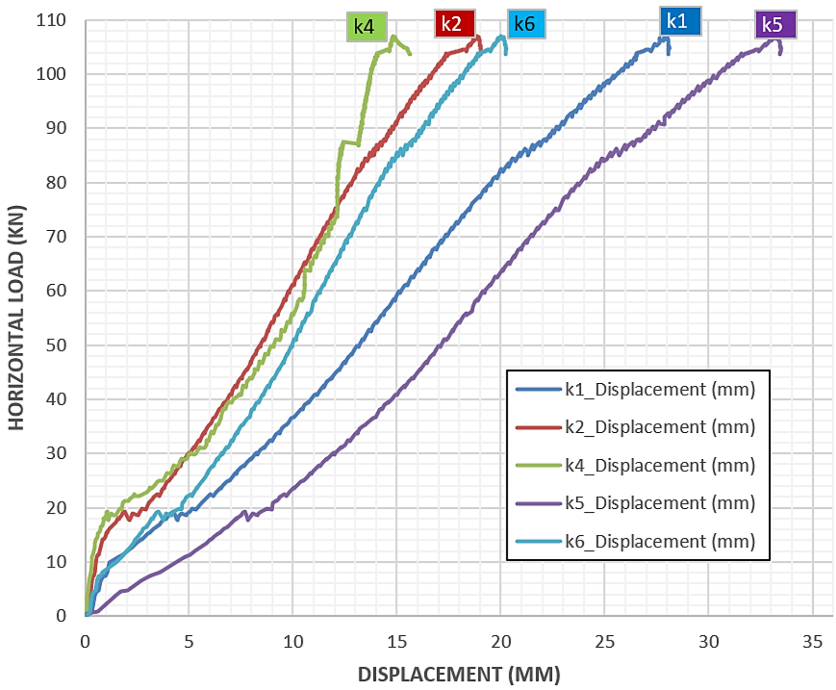

a) TGD1 wall

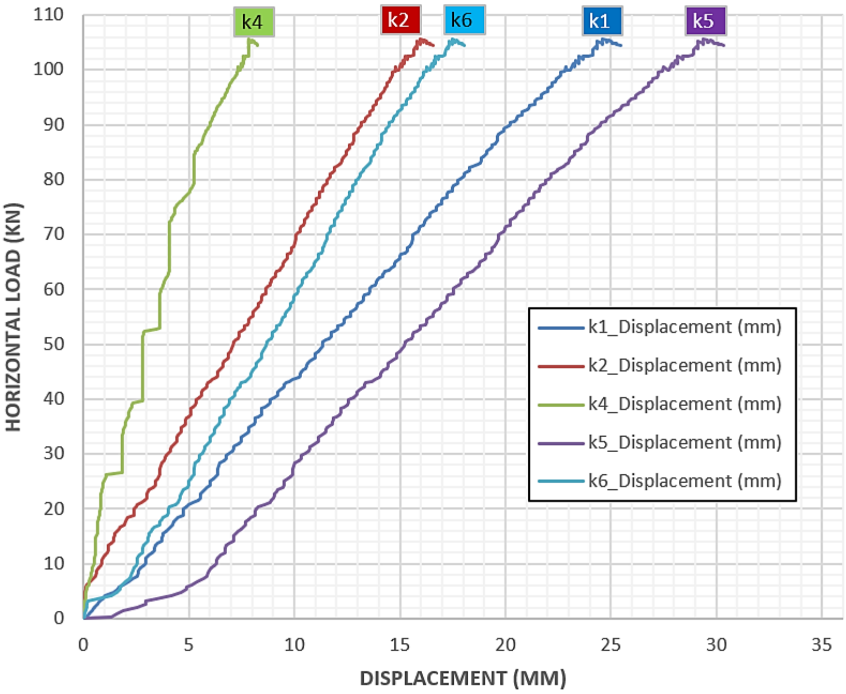

b) TGD2 wall

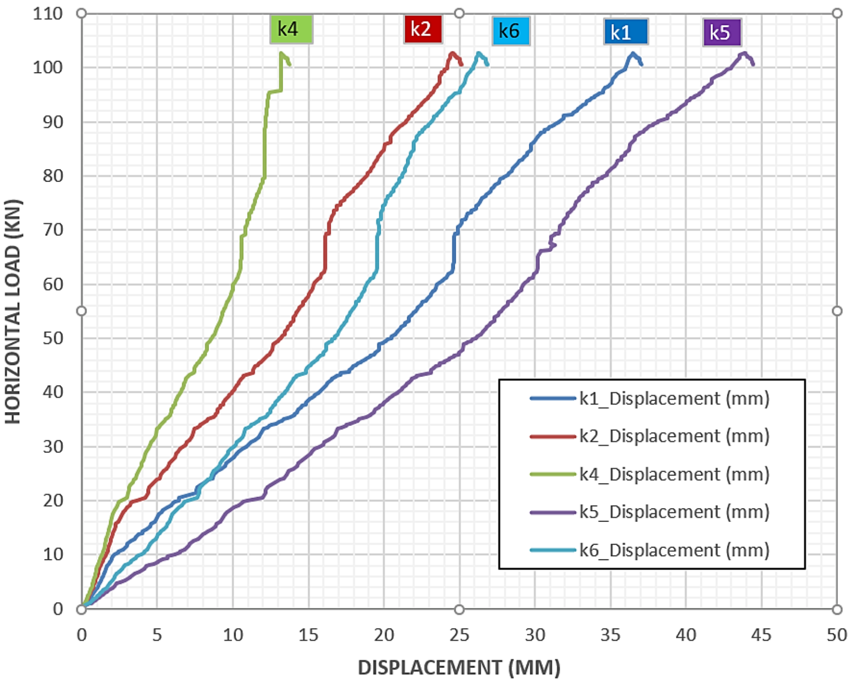

c) TGD3 wall

Figure 14. Horizontal load-displacement graphs for one-sided reinforced walls

The maximum displacement occurred at the k5 displacement gauge. Horizontal load-displacement curves for the k5 displacement gauge of 6 samples are presented together in the graph below (Figure 15).

The average peak load obtained from the failure of the unreinforced walls was calculated as 33.28kN. On the other hand, the average peak load obtained from the failure of one-sided reinforced walls was 105.07 kN. This represents a 215.73% increase in strength for one-sided reinforced walls compared to unreinforced walls (Table 3).

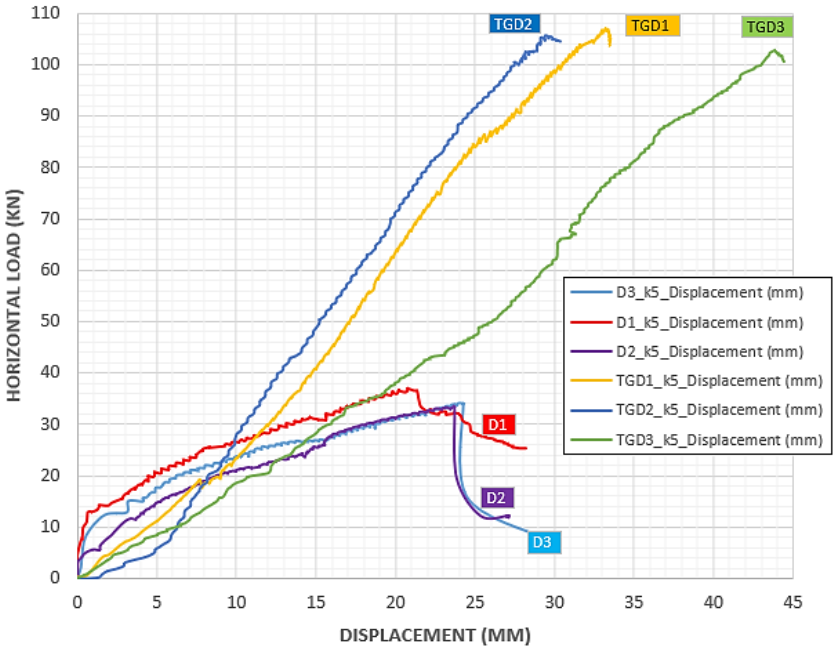

Figure 15. k5 displacement gauge D1-D2-D3-TGD1-TGD2-TGD3 horizontal load-displacement curves

Table 3. Average peak load (shear force) increases of one-sided reinforced walls compared to unreinforced walls

Sample code	Horizontal load (kN)	Average load (kN)	Increase rate
D1	32.16		
D2	33.45	33.28	
D3	34.23		
TGD1	106.85		
TGD2	105.56	105.07	215.73%
TGD3	102.81		

The average maximum displacement measured by the k5 displacement gauge, where the largest displacement was obtained from the failure of the unreinforced walls, was calculated as 23.88 mm. Conversely, the average maximum strain, measured by the k5 displacement gauge, where the greatest displacement was obtained from the failure of the one-sided reinforced walls, was calculated as 35.53 mm. The displacement increased by 48.82% in one-sided reinforced walls compared to unreinforced walls (Table 4).

Table 4. Comparison of the displacement rate of one-sided reinforced walls versus unreinforced walls

Sample code	k5_displacement (mm)	Average displacement (mm)	Increase rate
D1	23.69		
D2	23.71	23.88	
D3	24.23		
TGD1	33.33		
TGD2	29.39	35.53	48.82%
TGD3	43.88		

4. The Shear Strength in the Masonry Walls

If the shear force is defined as V_d for a masonry wall with a cross-sectional area A_d, then the shear strength and cross-sectional area for masonry walls are;

$$A_d = b_d \times l_d \tag{1}$$

$$\tau_d = V_d / A_d \tag{2}$$

Here, if V_d represents the horizontal failure load of the walls obtained from the tests, the experimental shear strength value is determined. When calculating the cross-sectional area A_d, b_d is considered as the wall thickness and l_d as the wall length. While calculating A_d, the wall length for all walls is standardized to 150 mm. The wall thickness for unreinforced walls is set at 90 mm. In contrast, the wall thickness for single-sided reinforced walls is adjusted to 130 mm, taking into account the additional 40 mm thickness of the reinforcement mortar.

The horizontal failure load, which can be defined as the shear force on one-sided reinforced walls, increased by 215.73% compared to unreinforced walls, while the shear strength increased by 118.58% (Table 5).

Table 5. Experimental shear strength increase rate

Sample code	Shear strength τ_d (MPa)	Average shear strength τ_d (MPa)	Increase rate
D1	0.24		
D2	0.25	0.25	
D3	0.25		
TGD1	0.55		
TGD2	0.54	0.54	118.58%
TGD3	0.53		

4.1. Comparison of Experimental Shear Strengths of Walls with Literature

Standards and various empirical formulas in the literature were used to determine the wall shear strength. By comparing the shear capacities obtained from the test results with the values obtained from these standards, the damage conditions of the walls were evaluated and the test results were supported.

In the Turkish Building Earthquake Code of 2018 (TBDY-2018), the shear force strength of the infill wall reinforced with steel-mesh reinforcement will be considered as the horizontal component of the equivalent compressive force strength of the diagonal bar. The shear force strength V_d of the reinforced infill wall with cross-sectional area A_d, compressive strength f_d, and shear strength τ_d will be calculated with the following equation [26].

$$V_d = A_d\,(\tau_d + f_{yd}\,\rho_{sh}) \leq 0.22\,A_d\,f_d \tag{3}$$

Here, f_{yd} is the design yield strength of the mesh reinforcement, and ρ_{sh} is the ratio of the horizontal body reinforcements in the wall to the gross cross-sectional area of the wall. Mesh reinforcement has the same reinforcement area in horizontal and vertical directions. The calculation was made by taking the reinforcement area to zero in unreinforced plain walls.

Shear force strength calculation of brick walls according to Eurocode 6 can be calculated through the following equations [31].

$$V_d = \tau_d b_d l_d + 0.9 l_d \left(\frac{A_s f_s}{s_h}\right) \tag{4}$$

$$\tau_d = 0.2 + 0.4\left(\frac{P_d}{b_d l_d}\right) \tag{5}$$

Where; V_d: Shear force; τ_d: Wall shear strength; b_d: Wall thickness; l_d: Wall length; A_s: Reinforcement cross-sectional area; f_s: Yield strength of reinforcement; s_h: Horizontal reinforcement spacing (mm); and P_d: Vertical load.

Table 6. Shear capacity Vd (N) comparison of experimental results with standards

Sample code	Experimental data		Eurocode 6	TBDY-2018
D1	32.160		47.000	33.750
D2	33.450	33.280	47.000	33.750
D3	34.230		47.000	33.750
TGD1	106.850		115.520	111.550
TGD2	105.560	105.073	115.520	111.550
TGD3	102.810		115.520	111.550

The results obtained from the experimental data were compared with the values calculated from the shear force formulas in Eurocode-6 and TBDY-2018 standards. The experimental shear force on unreinforced walls was found to be 41.23% lower than Eurocode-6 and 1.41% lower than TBDY-2018. The experimental shear force on one-sided reinforced walls was found to be 9.94% lower than Eurocode-6 and 6.16% lower than TBDY-2018. The results obtained from the experimental data for reinforced walls are consistent with the calculations in the standards.

5. Normalized Graphs and Graphic Equations

The derivation of function equations by normalizing the load-displacement graphs allows the load-displacement relationship to be expressed mathematically. Petry et al. expressed that, mathematically, the stress-strain and shear-normal stress graphs in their studies to determine the strength of brick walls at different scales [32]. Similarly, normalized graphs and mathematical equations were created using the results of unreinforced walls in various studies [33]. Trendline graphs and graph equations were created for each wall group with linearly calculated trendlines. An equation was produced to show the relationship between load-displacement for each wall group in Figures 16 and 17.

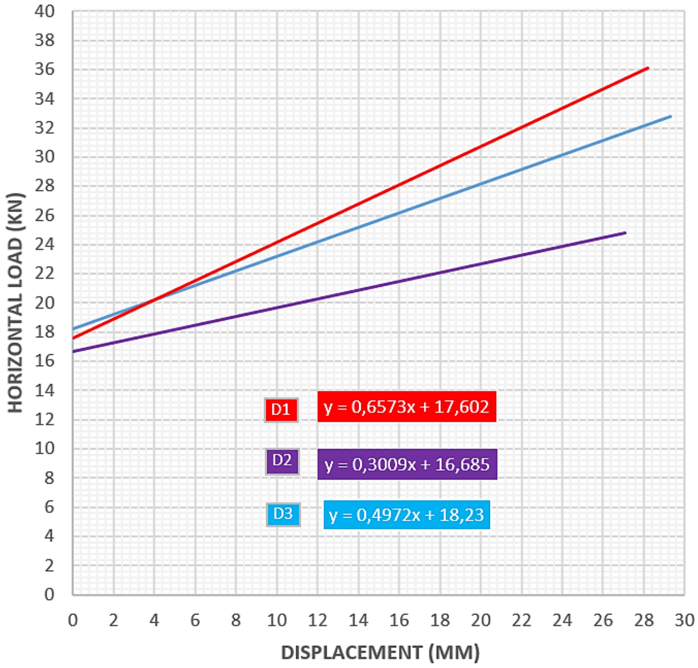

Figure 16. Unreinforced walls horizontal load (KN) - k5 displacement (mm) linear trendline graph and graph equations (D1-D2-D3)

P_D = Load applied to unreinforced walls

Δ_D = Unreinforced walls displacement value

$$P_D = 0.49\Delta_D + 17.51 \quad (6)$$

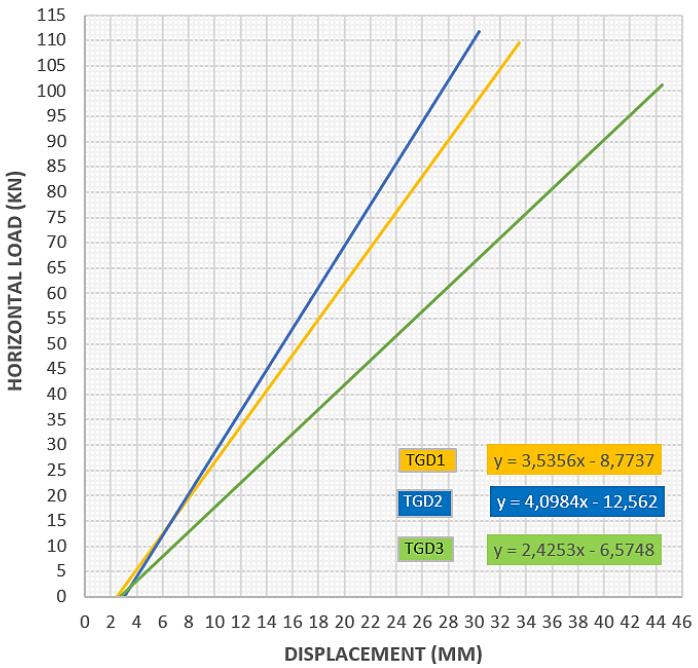

Figure 17. One-sided reinforced walls horizontal load (KN)- k5 displacement (mm) linear trendline graph and graph equations (TGD1-TGD2-TGD3)

P_{TGD} = Load applied to One-sided reinforced walls

Δ_{TGD} = One-sided reinforced walls displacement value

$$P_{TGD} = 3.35\Delta_{TGD} - 9.30 \quad (7)$$

6. Results and Discussion

The results presented in Table 3 and Figure 14 clearly demonstrate the impact of reinforcement on masonry wall samples. The one-sided reinforced walls exhibited an average peak load that was 215.73% higher than that of the unreinforced walls. Additionally, the average maximum displacement measured by the displacement gauge increased by 48.82% in one-sided reinforced walls compared to unreinforced walls. Furthermore, the one-sided reinforced walls displayed a shear strength increase of 118.58% higher than the unreinforced walls. These percentage results fall within the range reported by other researchers.

In the study conducted by Şimşek, which can be considered a smaller-scale wall sample compared to the current study, the vertical deformation values of undamaged walls strengthened on one side with Khorasan mortar reinforced with steel mesh increased by 21% compared to unreinforced walls. Additionally, the shear stresses of undamaged walls strengthened on one side with Khorasan mortar reinforced with steel mesh increased by 29% compared to unreinforced walls [15]. The current study exhibited better shear strength values than the study by Şimşek. However, it also showed higher vertical deformations. It's important to note that the larger size of the test samples and the diameter of the reinforcement used are significant factors affecting the results. In the study by Biolzi et al., reinforced and plastered masonry walls underwent cyclic diagonal compression loading under displacement control. These specimens were strengthened with steel-reinforced plasters of varying thicknesses, resulting in maximum loads between 162% and 188% higher than their corresponding unreinforced counterparts [9]. While Lubin et al. [13] achieved an increased capacity of approximately 84%, Moeini et al. [10] reported an increase in the lateral in-plane capacity of the URM wall by approximately 115% in the presence of a vertical load.

In the study by ElGawady et al., the calculated shear strengths ranged from approximately 99% to 177% of the measured lateral resistances [23]. Ismail et al. determined that shear strength increases range from 128% to 136% in in-plane-loaded walls [24]. In the study by Wang et al., the average shear strength of unreinforced panels resulted in shear strength increases of 121% and 78% for panels reinforced with a grid of symmetrical and bidirectional strips. Simultaneously, panels with only horizontal reinforcement exhibited a moderate increase in shear strength of 94% and 72%, while panels with only vertical reinforcement exhibited a lower increase of 48% and 30% [19]. In the study by Garcia-Ramonda et al., regarding the overall performance, specimen LDS_2 demonstrated a substantial improvement in lateral load-bearing capacity with SRG containing one layer of LDS, achieving a peak load 42% greater than the corresponding value for URM walls. This percentage represents the average of the peak loads obtained for both directions. This specimen also exhibited a remarkable improvement of about 90% in displacement capacity compared to URM walls. Regarding the overall performance, the SRG with two layers of LDS exhibited, on average, a remarkable increment in both lateral load bearing and displacement capacity, with increases of 59% and 89%, respectively, compared to URM specimens [18].

In the study by Torunbalci et al., increases in the load-bearing capacities were determined to be 100% and 170%, respectively, in walls reinforced with standard concrete and self-compacting concrete [16]. In the Torunbalci et al. study, the increase in the load-bearing capacities of the one-sided reinforced wall samples was approximately 100%. On the other hand, this ratio was 135% on average for the one-sided reinforced wall that had previously been damaged [17]. Parisi et al. indicate that FRCM systems applied to URM walls subjected to diagonal compression can result in a shear strength increase ranging from 36% to 441%, along with an increase in pseudo-ductility ranging from 10% to 130%. Furthermore, the load and displacement capacities of FRCM-strengthened walls subjected to shear-compression loading can increase by approximately 12% to 30% and 14% to 83%, respectively. This wide range can be attributed to the fact that the lower the capacity of as-built masonry, the greater the capacity increase achievable with the FRCM [34]. The strength increase values in the current study fall within the ranges reported in existing literature.

The studies on reinforced masonry walls were examined, and the 10 related studies were classified in terms of the test method, reinforcement mortar, reinforcement material, capacity increase, and one-sided or two-sided reinforcements (Table 7). The strength increase of one-sided reinforced samples ranges from 29% to 170%, while the strength increase of two-sided reinforced samples falls within the range of 42% to 248%. The strength increase for samples reinforced with only one-sided steel mesh varies between 29% and 121%. The 118.58% strength increase value in this study falls within the range of strength increase for one-sided reinforced samples in the table. When reviewing all the studies in the table, it becomes evident that, on average, the strength increase in two-sided reinforced walls is approximately twice as good as that in one-sided reinforced walls.

In our study, the Diagonal Compression Test technique was used in six studies, while the Shear Compression Test technique was used in four studies. Upon analyzing the strength results, it became evident that the difference in the test method did not impact the increase in shear capacity. However, as the sample size increases, the application of the Diagonal Compression Test technique becomes progressively challenging. Conversely, the Shear Compression Test technique can be applied to larger samples, allowing for measurements from multiple points. In our study, measurements were taken using a five-point displacement meter, enabling a more precise assessment of the lateral displacement of the walls. In addition, this test system provides a more realistic simulation of the lateral load generated by seismic forces.

The use of cementitious mortar and lime-based mortar increased the strength capacity in all studies. However, there was no statistically significant difference between them. The types of strengthening materials used in mortars are presented in the table. Steel-based materials (steel mesh, steel sheets, and steel cords) were used in 7 studies, while various fiber materials were used in the other 4 studies. There was no clear advantage in terms of strength increase between the strengthening materials.

In Table 7, the test results are compared with the shear forces calculated according to the methods specified in the regulations. While making the calculations, the horizontal cross-sectional area was determined as the cross-sectional area of the brick for the unreinforced walls. For the reinforced walls, the horizontal cross-sectional area was calculated as the sum of the cross-sectional area of the brick and reinforcement plaster thickness. The test results are consistent with the values obtained from the regulations. The test results align with the values obtained from the regulations, particularly showing greater compatibility with the TBDY-2018 standard.

In Figures 15 and 16, load-displacement graphs were converted into normalized graphs, and derivative equations were generated. These equations enable the definition of the relationship between load and displacement.

This study offers several contributions to the existing community. The strengthening system utilizing Khorasan mortar with steel-mesh reinforcement, containing lime-based natural pozzolan, provides the following advantages. Most strengthening mortars available on the market generally contain cement. However, the reinforcement mortar used in this study contains natural pozzolan and lime. Its cement-free composition distinguishes it as a reinforcement system that will not cause any chemical damage to existing masonry bricks and lime mortars, especially in historical buildings. The reinforcement mortar used in the study was designed to be compatible with the composition of Khorasan mortar in existing buildings, enhancing the interface relationship between old and new materials in terms of strength. The incorporation of mesh reinforcement in the plaster has led to a more ductile fracture behavior, addressing a significant issue in masonry structures—brittle fractures. In the literature, studies on the strengthening of masonry walls have typically examined waiting periods of up to 12 months at most. This study, however, represents a significant advancement by investigating the long-term effects of reinforcement on masonry walls through a 24-month waiting period.

Table 7. Experimental test results on strengthened masonry specimens in the literature

Reference	Test Method	Reinforcement mortar	Strengthening Material	Capacity increase (%)
Şimşek et al. [15]	Diagonal compression test	Lime-based mortar	Steel mesh (one-sided reinforcement)	29
			Steel mesh (one-sided reinforcement)	75
Biolzi et al. [9]	Diagonal compression test	Lime-cement mortar	Steel mesh (two-sided reinforcement)	162 - 188
Lubin et al. [13]	Shear compression test	Cementitious mortar	Welded wire mesh (two-sided reinforcement)	84
Moeini et al. [10]	Shear compression test	Cementitious mortar	Steel mesh (one-sided reinforcement)	115
Wang et al. [19]	Diagonal compression test	Cementitious mortar	Steel cord (Symmetrical and bidirectional strips) (two-sided reinforcement)	78 - 121
			Steel cord (Only horizontal strips) (two-sided reinforcement)	72 - 94
Garcia-Ramonda et al. [18]	Shear compression test	Lime-based mortar	Low-density steel sheets (One Layer) (two-sided reinforcement)	42
			Low-density steel sheets (Two Layer) (two-sided reinforcement)	59
ElGawady et al. [23]	Shear compression test	No mortar (epoxy adhesive)	Carbon FRP- Glass FRP textile (one-sided reinforcement)	100 to 170
Torunbalci et al. [16]	Diagonal compression test	No mortar (epoxy adhesive)	Carbon FRP strips (one-sided reinforcement)	100
D'antino et al. [8]	Diagonal compression test	Lime-based mortar	Glass FRP (two-sided reinforcement)	248 - 220
Dehghani et al. [35]	Diagonal compression test	Cementitious mortar	PVA fibers (one-sided reinforcement)	55
			PVA fibers (two-sided reinforcement)	160

7. Conclusions

The experimental program presented in this paper primarily focused on the in-plane response of masonry walls strengthened with steel-mesh-reinforced Khorasan plaster. The evaluation of the walls was carried out through in-plane horizontal loading tests. A comparative analysis was performed between unreinforced and reinforced walls to assess the effectiveness of the reinforcement system. The following conclusions can be drawn from this experimental study:

- A significant increase in strength was observed in the samples reinforced with one-sided steel-mesh-reinforced Khorasan plaster compared to the unreinforced samples. This finding aligns with the results of similar strengthening studies conducted with cement mortar in the existing literature. Unreinforced walls exhibited a more brittle fracture behavior, while reinforced walls displayed a more ductile fracture behavior.
- The reinforcement systems applied to one side of the masonry walls induced secondary out-of-plane bending deformations, leading to distinct fracture patterns on the non-reinforced and reinforced surfaces of the walls. While diagonal fractures occurred on the non-reinforced surface, grid cracks formed at the mesh reinforcement lines.
- Upon examining the present study and other relevant studies in the literature, it is evident that walls strengthened with steel-mesh-reinforced Khorasan mortar exhibited more ductile behavior compared to unreinforced walls. Additionally, in the literature, masonry walls reinforced with FRP tend to exhibit a more brittle behavior than walls strengthened with steel-mesh-reinforced mortars.
- The Khorasan reinforcement mortar with steel-mesh reinforcement forms a robust connection and effectively interacts with the wall. There was no significant delamination observed at the interface between the reinforcement mortar and the wall until the wall ruptured. Even after the fracture, there was no separation except for a minor fragmentation in the area where the load was applied.
- During the design of the experimental setup, certain rotations were observed, particularly at the lower points of the test samples, despite the inclusion of measures to mitigate out-of-plane movements. While these rotations did not detrimentally affect the test results, it is advisable to consider additional mechanisms to prevent such rotations in the examination of larger dimensions or thicker walls.
- In comparing the results of this study to findings in the existing literature, it becomes evident that the use of cementitious mortar or lime-based mortar does not exhibit a statistically significant advantage over each other in terms of the increase in strength. However, in these studies, the incorporation of pozzolana and/or high-quality lime to increase the strength of the lime-based mortars used for reinforcement has proven effective in achieving higher levels of strength.
- The test method to be chosen according to the sample size is important for ease of application. The Diagonal Compression Test technique is preferred for its quick setup and faster experimentation. Additionally, it also facilitates the prevention of out-of-plane rotations in these experimental setups. However, as the sample size increases, the weight and difficulty of placing larger samples in this setup become more pronounced. Additionally, this test setup only allows data collection from strain gauges placed in two diagonal directions. In contrast, the Shear Compression Test setup is more suitable for larger and more comprehensive samples, permitting the testing of larger specimens. Furthermore, it allows the placement of multiple strain gauges in various directions. Nevertheless, it is more challenging to implement mechanisms to prevent out-of-plane movements in this setup, and its production costs are higher. Thus, these factors should be taken into consideration when choosing the appropriate experimental setup for the intended experiment.

Advancements in material science facilitate the ongoing development of new and environmentally friendly materials with reduced chemical footprints. This presents opportunities for researching new and cost-effective methods to fortify existing masonry structures using these materials. In future studies, comprehensive literature reviews can be conducted to categorize the various approaches employed for masonry wall strengthening. Such endeavors can guide the determination of the most efficacious and economical methods for reinforcement.

8. Declarations

8.1. Author Contributions

Conceptualization, V.O. and N.T.; methodology, V.O. and N.T.; software, V.O.; validation, V.O. and N.T.; formal analysis, V.O. and N.T.; investigation, V.O. and N.T.; resources, V.O. and N.T.; data curation, V.O. and N.T.; writing—original draft preparation, V.O. and N.T.; writing—review and editing V.O.; visualization, V.O.; supervision, V.O. and N.T.; project administration, V.O. and N.T. All authors have read and agreed to the published version of the manuscript.

8.2. Data Availability Statement

The data presented in this study are available in the article.

8.3. Funding

The authors received financial support for the resea-rch from Istanbul Technical University (ITU) Scientific Research Projects Department (Project No: 39657).

8.4. Conflicts of Interest

The authors declare no conflict of interest.

9. References

[1] Kashani, H. K., Shakiba, M., Bazli, M., Hosseini, S. M., Mortazavi, S. M. R., & Arashpour, M. (2023). The structural response of masonry walls strengthened using prestressed near surface mounted GFRP bars under cyclic loading. Materials and Structures, 56, 112. doi:10.1617/s11527-023-02201-0.

[2] Monaco, A., Minafò, G., Cucchiara, C., D'Anna, J., & La Mendola, L. (2017). Finite element analysis of the out-of-plane behavior of FRP strengthened masonry panels. Composites Part B: Engineering, 115, 188–202. doi:10.1016/j.compositesb.2016.10.016.

[3] Torres, N., Tumialan, J. G., Nanni, A., Bennet, R. M., & De Caso Basalo, F. J. (2022). Flexural Design of Masonry Walls Reinforced with FRP Bars Based on Full-Scale Structural Tests. American Concrete Institute, ACI Special Publication, SP-356, 291–311. doi:10.14359/51737277.

[4] Dong, Z., Deng, M., Dai, J., & Ma, P. (2021). Diagonal compressive behavior of unreinforced masonry walls strengthened with textile reinforced mortar added with short PVA fibers. Engineering Structures, 246. doi:10.1016/j.engstruct.2021.113034.

[5] Castori, G., Corradi, M., & Sperazini, E. (2021). Full size testing and detailed micro-modeling of the in-plane behavior of FRCM–reinforced masonry. Construction and Building Materials, 299. doi:10.1016/j.conbuildmat.2021.124276.

[6] Vienni, C., Salvatori, L., & Orlando, M. (2022). Cyclic shear-compression tests on CRM reinforced brick masonry walls. Procedia Structural Integrity, 44, 2262–2269. doi:10.1016/j.prostr.2023.01.289.

[7] Vienni, C., Orlando, M., & Salvatori, L. (2022). CRM reinforced brick masonry walls: Experimental and parametric numerical investigations. Procedia Structural Integrity, 44, 2270–2277. doi:10.1016/j.prostr.2023.01.290.

[8] D'Antino, T., Carozzi, F. G., & Poggi, C. (2019). Diagonal shear behavior of historic walls strengthened with composite reinforced mortar (CRM). Materials and Structures, 52, 114. doi:10.1617/s11527-019-1414-1.

[9] Biolzi, L., Cattaneo, S., Crespi, P., Scamardo, M., & Vafa, N. (2023). Diagonal compression cyclic testing of unreinforced and reinforced masonry walls. Construction and Building Materials, 363. doi:10.1016/j.conbuildmat.2022.129839.

[10] Ehteshami Moeini, M., Razavi, S. A., Yekrangnia, M., Pourasgari, P., & Abbasian, N. (2022). Cyclic performance assessment of damaged unreinforced masonry walls repaired with steel mesh reinforced shotcrete. Engineering Structures, 253. doi:10.1016/j.engstruct.2021.113747.

[11] Warjri, T., Marbaniang, D. F., & Marthong, C. (2022). In-plane behaviour of masonry walls embedding with steel welded wire mesh overlay with mortar. Journal of Structural Integrity and Maintenance, 7(3), 177–187. doi:10.1080/24705314.2022.2048241.

[12] Ullah, S., Farooq, S. H., Usman, M., Ullah, B., Hussain, M., & Hanif, A. (2022). In-Plane Seismic Strengthening of Brick Masonry Using Steel and Plastic Meshes. Materials, 15(11), 4013. doi:10.3390/ma15114013.

[13] Lubin, C., Guerrero, H., Alcocer, S. M., & Lopez Batiz, O. (2023). Experimental Behavior of Confined Masonry Walls Rehabilitated with Reinforced Mortar Jacketing Subjected to Cyclic Loading. Buildings, 13(5), 1314. doi:10.3390/buildings13051314.

[14] Hasnat, A., Ahsan, R., & Yashin, S. M. (2022). Quasi-static in-plane behavior of full-scale unreinforced masonry walls retrofitted using ferro-cement overlay. Asian Journal of Civil Engineering, 23(5), 649–664. doi:10.1007/s42107-022-00447-7.

[15] Şimşek, E. T. (2018). An Experimental Assessment of Textile and Wire Reinforced Horasan Mortar Strengthening of Brick Walls In Historical Buildings. MS.c. Thesis, I.T.U. Institute of Science and Technology, Istanbul, Turkey.

[16] Torunbalci, N., Ediz, I., & Sutcu, F. (2012). Strengthening a heritage structure with self-compacting concrete: An experimental study. WIT Transactions on State-of-the-art in Science and Engineering, 121. doi:10.2495/978-1-84564-754-4/11.

[17] Torunbalci, N., Onar, E., & Sutcu, F. (2011). An experimental study on alternative CFRP retrofitting applications of heritage structures. International Journal of Sustainable Development and Planning, 6(2), 152–165. doi:10.2495/SDP-V6-N2-152-165.

[18] Garcia-Ramonda, L., Pelà, L., Roca, P., & Camata, G. (2022). Experimental cyclic behaviour of shear masonry walls reinforced with single and double layered Steel Reinforced Grout. Construction and Building Materials, 320. doi:10.1016/j.conbuildmat.2021.126053.

[19] Wang, X., Lam, C. C., & Iu, V. P. (2018). Experimental investigation of in-plane shear behaviour of grey clay brick masonry panels strengthened with SRG. Engineering Structures, 162, 84–96. doi:10.1016/j.engstruct.2018.02.027.

[20] Özsaraç, S. (2009). The Experimental Investigatıon of Constructive Brick Walls Strengthened With Glass Fiber Reinforced Polymer in Masonry Buildings. MSc Thesis, I.T.U. Institute of Science and Technology, Istanbul, Turkey.

[21] Son, S. H., An, J. H., Song, J. H., Hong, Y. S., Jang, H. S., & Eun, H. C. (2021). In-plane strengthening of unreinforced masonry walls by glass fiber-reinforced polyurea. Civil Engineering Journal (Iran), 7(12), 2119–2129. doi:10.28991/cej-2021-03091782.

[22] Khan, I., Gul, A., Shahzada, K., Khan, N. A., Rehman, F. U., Samiullah, Q., & Khattak, M. A. (2021). Computational seismic analysis of dry-stack block masonry wall. Civil Engineering Journal (Iran), 7(3), 488–501. doi:10.28991/cej-2021-03091668.

[23] ElGawady, M. A., Lestuzzi, P., & Badoux, M. (2005). Aseismic retrofitting of unreinforced masonry walls using FRP. Composites Part B: Engineering, 37(2–3), 148–162. doi:10.1016/j.compositesb.2005.06.003.

[24] Ismail, N., & Ingham, J. M. (2016). In-plane and out-of-plane testing of unreinforced masonry walls strengthened using polymer textile reinforced mortar. Engineering Structures, 118, 167-177. doi:10.1016/j.engstruct.2016.03.041.

[25] Shermi, C., & Dubey, R. N. (2018). In-plane behaviour of unreinforced masonry panel strengthened with welded wire mesh and mortar. Construction and Building Materials, 178, 195–203. doi:10.1016/j.conbuildmat.2018.04.081.

[26] Kuterdem, K., Nurlu, M., Tekin, B. M., & Erbay, S. (2013). National Framework In Order To Reduce Earthquakes by Multistakeholder Participation in Turkey: National Earthquake Strategy and Action Plan of Turkey (UDSEP-2023), Turkey.

[27] ASTM E519/E519M-15. (2020). Standard Test Method for Diagonal Tension (Shear) in Masonry Assemblages. Book of Standards Volume: 04.05, 1-5. doi:10.1520/E0519_E0519M-15.

[28] Ashurst, J., & Ashurst, N. (1988). Practical Building Conservation-Mortars, Plasters and Renders. Ashgate Publishing, Farnham, United Kingdom.

[29] Price, C. (1984). Mortars, Cements and Grouts Used in the Conservation of Historic Buildings. Studies in Conservation, 29(1), 52. doi:10.2307/1505946.

[30] Moropoulou, A., Bakolas, A., Moundoulas, P., Aggelakopoulou, E., & Anagnostopoulou, S. (2002). Design and evaluation of restoration mortars for historic masonry using traditional materials and production techniques. Materials Research Society Symposium - Proceedings, 712, 77–82. doi:10.1557/proc-712-ii2.7.

[31] EN 1996-1-1. (2005). Eurocode 6–Design of masonry structures–Part 1-1: general rules for reinforced and unreinforced masonry structures. European Committee for Standardization, Brussels, Belgium.

[32] Petry, S., & Beyer, K. (2014). Scaling unreinforced masonry for reduced-scale seismic testing. Bulletin of Earthquake Engineering, 12(6), 2557–2581. doi:10.1007/s10518-014-9605-1.

[33] Parisi, F., Lignola, G. P., Augenti, N., Prota, A., & Manfredi, G. (2011). Nonlinear Behavior of a Masonry Subassemblage Before and After Strengthening with Inorganic Matrix-Grid Composites. Journal of Composites for Construction, 15(5), 821–832. doi:10.1061/(asce)cc.1943-5614.0000203.

[34] Parisi, F., Menna, C., & Prota, A. (2018). Fabric-reinforced cementitious matrix (FRCM) composites: Mechanical behavior and application to masonry walls. Failure Analysis in Biocomposites, Fibre-Reinforced Composites and Hybrid Composites, 199–227. doi:10.1016/B978-0-08-102293-1.00010-3.

[35] Dehghani, A., Fischer, G., & Nateghi Alahi, F. (2015). Strengthening masonry infill panels using engineered cementitious composites. Materials and Structures, 48, 185-204. doi:10.1617/s11527-013-0176-4.